

Optical Interferometric Observations of θ^1 Orionis C from NPOI and Implications for the System Orbit

J. Patience¹, R. T. Zavala², L. Prato³, O. Franz³, L. Wasserman³, C. Tycner⁴, D. J. Hutter², C. A. Hummel⁵

ABSTRACT

With the Navy Prototype Optical Interferometer (NPOI), the binary system θ^1 Orionis C, the most massive member of the Trapezium, was spatially resolved over a time period extending from February 2006 to March 2007. The data show significant orbital motion over the 14 months, and, after combining the NPOI data with previous measurements of the system from the literature, the observations span 10 years of the orbit. Our results indicate that the secondary did not experience an unusually close periastron passage this year, in contradiction to the prediction of a recently published, highly eccentric ~ 11 year orbit. Future observations of this source will be required to improve the orbital solution. Possible implications of the results in terms of system distance are discussed, although a main conclusion of this work is that a definitive orbit solution will require more time to obtain sufficient phase coverage, and that the interaction effects expected at periastron did not occur in 2007.

Subject headings: binaries: close; open clusters and associations: individual (Trapezium); stars: individual (θ^1 Orionis C); techniques: interferometric

¹University of Exeter, School of Physics, Astrophysics Group, Stocker Road, Exeter, EX4 4QL United Kingdom; patience@astro.ex.ac.uk

²U.S. Naval Observatory, Flagstaff Station, 10391 W. Naval Obs. Rd., Flagstaff, AZ 86001; bzavala@nofs.navy.mil; djh@nofs.navy.mil

³Lowell Observatory, 1400 West Mars Hill Rd., Flagstaff, AZ 86001; lprato@lowell.edu; otto.franz@lowell.edu; lhw@lowell.edu

⁴Department of Physics, Central Michigan University, Mt. Pleasant, MI 48859; c.tycner@cmich.edu

⁵European Southern Observatory, Karl-Schwarzschild-Str. 2, 85748 Garching, Germany; chummel@eso.org

1. Introduction

Orion is the nearest example of a giant molecular cloud and is the site of both high-mass star formation and a prodigious number of recently-formed stars; the central 2.5 pc region of the Orion Nebula Cluster (ONC) alone contains ~ 3500 stars with a combined mass exceeding $900 M_{\odot}$ (Hillenbrand 1997). Although star-forming regions such as Taurus are closer, these regions are dark clouds associated with low-mass star formation and far fewer total stars. Initial star-count studies (Lada et al. 1991) implied that up to 95% of stars formed in clustered environments like Orion, while more recent *Spitzer Space Telescope* results indicate that at least half of all stars originate in dense regions (Megeath et al. 2004). An analysis of binary star distributions (Patience et al. 2002) suggests that approximately 70% of field stars may have formed in a clustered environment. Thus, the study of Orion, the closest giant star forming cluster, is central to investigating the early history of the majority of stars. Furthermore, the variety of cluster morphologies investigated with *Spitzer* observations suggest that OB stars play a significant role in the formation and evolution of star formation in clusters (Megeath et al. 2004).

The distance to Orion is a critical parameter that influences the interpretation of many of the properties of the region and its members. Measurements range from ~ 390 pc to ~ 480 pc using a variety of methods and assumptions including observations of water masers, radio sources, an eclipsing binary, and statistical analysis (Genzel et al. 1981; Stassun et al. 2004; Sandstrom et al. 2007; Menten et al. 2007; Jeffries 2007, and references therein). A closer distance would imply that the stars are less luminous, and members that are still contracting onto the main sequence are consequently older based on comparison with theoretical evolutionary tracks (e.g., Siess et al. 2000; Palla & Stahler 1999). Older ages for the stars above the main sequence suggest a spread in ages.

Binary stars yield a model-independent distance with the combination of a spatially resolved orbit and a double-lined radial velocity orbit (e.g., Torres et al. 1997). Given the distance to Orion, very high angular resolution is required to separate binary systems which exhibit significant orbital motion. The binary system θ^1 Ori C (HD 37022) in the Trapezium region of Orion has such a close separation that it was not detected until speckle observations barely resolved the pair (Weigelt et al. 1999) with a separation of less than the diffraction limit of the 6m telescope employed in the discovery. The separation has decreased over time and is now best monitored with interferometry; a recent orbit fit suggested the system might be just past periastron and completing an orbital cycle within a year (Kraus et al. 2007). In this letter, we present the results of interferometric observations with NPOI that add significantly to the binary orbit phase coverage and suggest the orbital period may be substantially longer than predicted.

The distance to θ^1 Ori C in particular and its physical parameters such as mass and age are of great importance since the O7 primary (e.g., Garmany et al. 1982), as the most massive member of the ONC, has the dominant role in shaping the properties of the surrounding nebula, and strongly impacts the circumstellar material around the ONC stars. The photoionizing radiation from θ^1 Ori C produces the brightening of many proplyds (O’Dell et al. 1993), but also causes the material to escape. Observations of mass loss rates (Johnstone et al. 1998; Henney & O’Dell 1999) and theoretical modeling of the results (e.g., Stoerzer & Hollenbach 1999) imply that these structures cannot survive for $\gtrsim 10^5$ yrs, substantially less than the $<1-2$ Myr age of the ONC (Hillenbrand 1997). Possible explanations for the apparent contradiction in disk lifetimes and stellar ages include radial orbits for the proplyds (Stoerzer & Hollenbach 1999) or a very young age for θ^1 Ori C, such as has been proposed for θ^1 Ori B (Palla & Stahler 2001). In contrast, recent models of the evolution of disk sizes in the ONC (Clarke 2007) suggest that disk survival times of 1-2 Myr in the uv field produced by θ^1 Ori C are possible – consistent with the age of the stellar population. Key to estimating the age of θ^1 Ori C is placing the secondary accurately on the H-R diagram with a well-measured distance, luminosity, and mass given that the primary has already contracted onto the main sequence. We present new magnitude differences which will aid in the assessment of the luminosity, but concentrate on the orbital motion which is required to estimate the distance.

2. Observations and Data Reduction

During Feb. 2006 to Mar. 2007, θ^1 Ori C was observed with NPOI on 6 nights. The NPOI array at Anderson Mesa near Flagstaff, AZ, consists of six 50 cm (12 cm clear aperture) siderostats which can be deployed along a Y-shaped array of vacuum light pipes (Armstrong et al. 1998). The wavelength coverage spans 550–850 nm over 16 spectral channels. Details regarding the NPOI observational setup and data recording can be found in Hummel et al. (2003) and Benson et al. (2003). More recent upgrades relevant to this program are improvements in the acquisition camera sensitivity and calibration of the bias level for low count rates; implementation of these two changes enabled the observations of θ^1 Ori C. Table 1 provides a log of the NPOI observations.

The observations of θ^1 Ori C were interleaved with ϵ Ori, one of the bright ($V=1.70$) belt stars. The visibilities from ϵ Ori serve to calibrate both variable atmospheric conditions and the system response to a point source. The small angular diameter of ϵ Ori – 0.86 ± 0.16 milli-arcseconds (mas) (Mozurkewich et al. 1991) – and its proximity to θ^1 Ori C – less than 5° separation – allowed for accurate atmospheric correction. For both the target and

calibrator, the fringes were recorded in 2 ms frames for a total scan duration of 30 s before switching to the other source. The individual 2 ms data were averaged over a 1 s time period, and these 1 s data points were checked for outliers before averaging to generate 30 s averaged V^2 measurements. Calibration factors were determined by comparing the observed data of ϵ Ori to that expected from a 0.86 mas diameter single star. These calibration factors were then applied to observations of θ^1 Ori C. The flagging, averaging, and calibration steps were performed with the OYSTER package, as described in Hummel et al. (1998, 2003), except that the bias corrections were determined for each star individually.

3. Results and Analysis

The calibrated visibilities were fit with a model comprised of two stars with slightly resolved stellar surfaces. The primary star diameter was estimated to be 0.3 mas using the expected diameter of an O7 star at a distance of 450 pc (Drilling & Landolt 2000). Assuming the spectral type from Kraus et al. (2007), the secondary diameter was set to half that of the primary, rounded to 0.2 mas. The observational setup did not allow us to fit for such small diameters convincingly, so we held these values constant. Figure 1 shows examples of calibrated V^2 values and the best fit model. Predicted visibilities from a recent orbit solution (Kraus et al. 2007) are also plotted. Table 1 lists the epoch, siderostats used, number of baselines, maximum baseline length, number of scans, estimated separation and position angle with uncertainties, and the position error ellipses. Because each scan yields up to 16 V^2 values per baseline and up to 405 V^2 points were obtained during a night, individual measurements are not listed, but examples are plotted in Figure 1. Model fits to individual baselines include a 180° ambiguity in the position angle, and the values listed in Table 1 are chosen based on previous measurements and the inability to fit orbits if the companion was located in the opposite quadrant in the 2007 data. Some nights listed in Table 1 included closure phase observations, but we defer discussion of these results, which have the ability to directly resolve the 180° ambiguity, for a future paper including results from calibration binaries.

While the bandpass does not exactly match the V or R filters, our magnitude difference measured at 550 nm closely approximates that of the V band (Zavala et al. 2007). Considering all the data, the best estimates for the observed magnitude differences are $\Delta \text{mag}_{550\text{nm}} = 1.3 \pm 0.3$ and $\Delta \text{mag}_{700\text{nm}} = 1.2 \pm 0.2$. The NPOI measurement agrees with previous ΔV estimates from speckle observations taken at the 6.0 m Special Astrophysical Observatory at Mt. Pastukhov in Russia (1.1 mag, Kraus et al. 2007).

Orbits based on the previous measurements and the new NPOI data are shown in Figure

2. The earliest NPOI data from Feb. 2006 show only minimal orbital motion from the IOTA Dec. 2005 data (Kraus et al. 2007), indicating there is not an offset between the two systems. The 2007 NPOI data show significant evolution in the orbit. The measured separations of the secondary relative to the primary are larger than expected from the predicted orbit and lag behind the solution in orbital phase (Kraus et al. 2007). The NPOI results indicate that a very close periastron passage did not take place this year as suggested by the preliminary orbital solutions of Kraus et al. (2007).

As indicated in Figure 2, only part of the orbit – probably less than one half – is covered by the extant data, making any assessment of the orbit fit preliminary. Combining all previous position measurements and associated error bars with the NPOI visibilities and uncertainties, we fit an orbit using ORBGRID (Hartkopf et al. 1989; Mason et al. 1999) and used its solution as a starting point for a least squares solution; uncertainties from the covariance matrix of the least squares solution are quoted (Table 2). Both ORBGRID and the least squares solution weight the astrometric points in a relative sense, and we set these weights according to the areas of the error ellipses from our Table 1 and Table 3 of Kraus et al. (2007).

We stress that the orbital elements of the best fit based on the current data (Table 2) may be modified substantially as more data become available. Compared with the previous solution, we find a longer period and a much less eccentric orbit. Our lower eccentricity of 0.16 is well within the bulk of the distribution for T Tauri binaries (e.g., Mathieu 1994), the lower mass counterparts of θ^1 Ori C. In contrast, the earlier solution found an extremely high eccentricity of 0.91–0.93 (Kraus et al. 2007).

Although it is premature to calculate a robust distance to the Orion Nebula Cluster from our data, if we assume a total system mass of $40 M_{\odot}$ the orbital elements in Table 2 give a dynamical parallax distance of 730 pc — unrealistically large considering the distance to the background high extinction molecular gas (Genzel et al. 1981). The $40 M_{\odot}$ value is the minimum mass estimate from the evolutionary tracks of Walborn & Nichols (1994), using a T_{eff} for an O7 star of 36,000 K (Massey et al. 2005). The values of $\Delta\text{mag}_{550\text{nm}}$ and $\Delta\text{mag}_{700\text{nm}}$ between the primary and secondary stars imply at the latest a B2 secondary spectral type (Drilling & Landolt 2000), with a corresponding T_{eff} of 28,000 K. Thus, $40 M_{\odot}$ is a lower limit; larger masses would imply an even greater distance.

Figure 3 summarizes our dynamical parallax measurement. The uncertainty in the value of a^3/P^2 (Table 2), directly related to parallax, does not yield a reliable estimate of distance at this time. Increasing the semi-major axis by 1σ and reducing the period by 1σ yields a low value for the distance of 344 pc for the same total mass. Clearly, the available data do not significantly constrain the distance to θ^1 Ori C. Figure 3 compares the best-fit semi-

major axis and period, with their associated 1σ and 2σ error ellipses, to the values expected for the two Orion distances estimated from the radio star and the maser. To explore fits to our data with more physical distances imposed, we selected a range of nine periods from 10 to 26 years and determined the corresponding semi-major axes for distances of 390 pc and 480 pc. For both distances, fits were obtained for periods of ~ 22 years with orbital elements that agreed to within $\sim 3\sigma$ of the best fit elements (Table 2). Fits for other periods were significantly (by many sigma) worse.

Further monitoring of the orbit of θ^1 Ori C is required to decrease the errors in the orbital elements and provide a reliable dynamical distance. Given the proximity to periastron passage, continued observations are particularly important over the next months and years. Resolving the distance and mass of θ^1 Ori C, and revealing the nature of its interactions with the local environment, will provide important insight into the closest region of massive star formation.

The Navy Prototype Optical Interferometer is a joint project of the Naval Research Laboratory and the US Naval Observatory, in cooperation with Lowell Observatory, and is funded by the Office of Naval Research and the Oceanographer of the Navy. The authors would like to thank Jim Benson and the NPOI observational support staff Dave Allen, Jim Clark, Brit O’Neill, Susan Strosahl, Dale Theiling, Josh Walton and Ron Winner whose efforts made this project possible. We thank Phil Massey, Nathan Mayne for helpful discussions, and Nat White for assistance with observing arrangements. RTZ thanks the Michelson Science Center for an invitation to visit which helped initiate this work, and JP gratefully acknowledges funding from the Michelson Fellowship Program.

Facilities: NPOI ()

REFERENCES

- Armstrong, J. T., et al. 1998, ApJ, 496, 550
- Benson, J.A., Hummel, C.A. & Mozurkewich, D. 2003, Proc. SPIE, 4838, 358
- Clarke, C. J. 2007, MNRAS, 376, 1350
- Drilling, J. S., & Landolt, A. U. 2000, in *Astrophysical Quantities*, ed. A. N. Cox (New York: Springer), 388–389
- Garmany, C. D., Conti, P. S., & Chiosi, C. 1982, ApJ, 263, 777

- Genzel, R., Reid, M. J., Moran, J. M., & Downes, D. 1981, *ApJ*, 244, 844
- Hartkopf, W. I., McAlister, H. A., & Franz, O. G. 1989, *AJ*, 98, 1014
- Henney, W. J. & O'Dell, C. R. 1999, *AJ*, 118, 2350
- Hillenbrand, L. A. 1997, *AJ*, 113, 1733
- Hummel, C. A., et al. 2003, *AJ*, 125, 2630
- Hummel, C. A., Mozurkewich, D., Armstrong, J. T., Hajian, A. R., Elias, N. M., II., & Hutter, D. J. 1998, *AJ*, 116, 2536
- Jeffries, R. D. 2007, *MNRAS*, 376, 1109
- Johnstone, D., Hollenbach, D., & Bally, J. 1998, *ApJ*, 499, 758
- Kraus, S., et al. 2007 *A&A*, 466, 649
- Lada, E. A., Evans, N. J., II., Depoy, D. L., & Gatley, I. 1991, *ApJ*, 371, 171
- Mason, B. D., Douglass, G. G., & Hartkopf, W. I. 1999, *AJ*, 117, 1023
- Massey, P., Puls, J., Pauldrach, A. W. A., Bresolin, F., Kudritzki, R. P., & Simon, T. 2005, *ApJ*, 627, 477
- Mathieu, R. D. 1994, *ARA&A*, 32, 465
- Megeath, S. T., et al. 2004, *ApJS*, 154, 367
- Menten, K. M., Reid, M. J., Forbich, J., & Brunthaler, A. 2007, *A&A*, 474, 515
- Mozurkewich, D., et al. 1991, *AJ*, 101, 2207
- O'Dell, C. R., Wen, Z., & Hu, X. 1993, *ApJ*, 410, 696
- Palla, F. & Stahler, S. W. 1999, *ApJ*, 540, 255
- Palla, F. & Stahler, S. W. 2001, *ApJ*, 553, 299
- Patience, J., Ghez, A. M., Reid, I. N., & Matthews, K. 2002, *AJ*, 123, 1570
- Sandstrom, K. M., Peek, J. E. G., Bower, G. C., Bolatto, A. D., & Plambeck, R. L. 2007, *ApJ*, 667, 1161
- Siess, L., Dufour, E., & Forestini, M., 2000, *A&A*, 358, 593

Stassun, K. G., Mathieu, R. D., Vaz, L. P. R., Stroud, N., & Vrba, F. J. 2004, *ApJS*, 151, 357

Stoerzer, H. & Hollenbach, D. 1999, *ApJ*, 515, 669

Torres, G., Stefanik, R. P., & Latham, D. W. 1997, *ApJ*, 479, 268

Walborn, N. R., & Nichols, J. S. 1994, *ApJ*, 425, L29

Weigelt, G., Balega, Y., Preibisch, T., Schertl, D., Schoeller, M., & Zinnecker, H. 1999, *A&A*, 347, L15

Zavala, R. T., et al. 2007, *ApJ*, 655, 1046

Table 1. NPOI Observations and V^2 Model Fit Results

UT Date (1)	Julian Year (2)	Siderostats (3)	# b.l. (4)	Max b.l. (5)	$\#V^2$ (6)	ρ (7)	σ_ρ (8)	θ (9)	σ_θ (10)	σ_{maj} (11)	σ_{min} (12)	σ_ϕ ($^\circ$) (13)
2006 Feb 24	2006.1486	AC-AE-AW	2	22.2	171	11.80	1.11	152.3	3.5	1.20	0.54	178.0
2007 Feb 22	2007.1425	AE-AW-W7	2	37.4	118	11.94	0.31	88.1	5.2	1.09	0.28	170.4
2007 Feb 25	2007.1507	AE-AW-W7	2	37.4	60	12.13	1.58	92.9	8.8	2.41	0.39	142.8
2007 Mar 06	2007.1753	AE-AW-AN-W7	4	38.1	405	12.17	0.37	86.6	2.1	0.46	0.36	157.6
2007 Mar 17	2007.2055	AE-AW-AN-W7	4	38.1	135	12.28	0.41	85.6	1.9	0.46	0.35	42.2
2007 Mar 20	2007.2137	AE-AW-AN-W7	4	38.1	200	12.14	0.43	83.0	2.3	0.49	0.42	158.2

Note. — Col. (1): UT date of NPOI observation Col. (2): Julian Year of NPOI observation. Col. (3): Siderostats used Col. (4): Number of independent baselines Col. (5): Max. baseline length (m) Col. (6): Number of V^2 measurements Col. (7): Fitted binary separation (mas) Col. (8): Error in ρ (mas) Col. (9): Fitted binary position angle ($^\circ$); this angle is chosen as it is a smooth extension of previous results and no orbital solutions could be found using $\theta + 180^\circ$ Col. (10): Error in θ ($^\circ$) Col. (11): Semi-major axis of error ellipse (mas). Col. (12): Semi-minor axis of error ellipse (mas) Col. 13: Position angle of error ellipse.

Table 2. ORBITAL ELEMENTS

Data	Value
a (mas)	41 ± 14
i (deg)	107.2 ± 3.5
Ω (deg)	208.8 ± 3.7
e	0.16 ± 0.14
ω (deg)	96.9 ± 118.7
T_0 (JY)	2007.0 ± 5.9
T_0 (JD)	2454101 ± 2154
P (days)	9497 ± 1461
P (years)	26 ± 13
a^3/P^2 (mas ³ /yr ²)	103 ± 146
χ^2/dof	2.6×10^{-6}

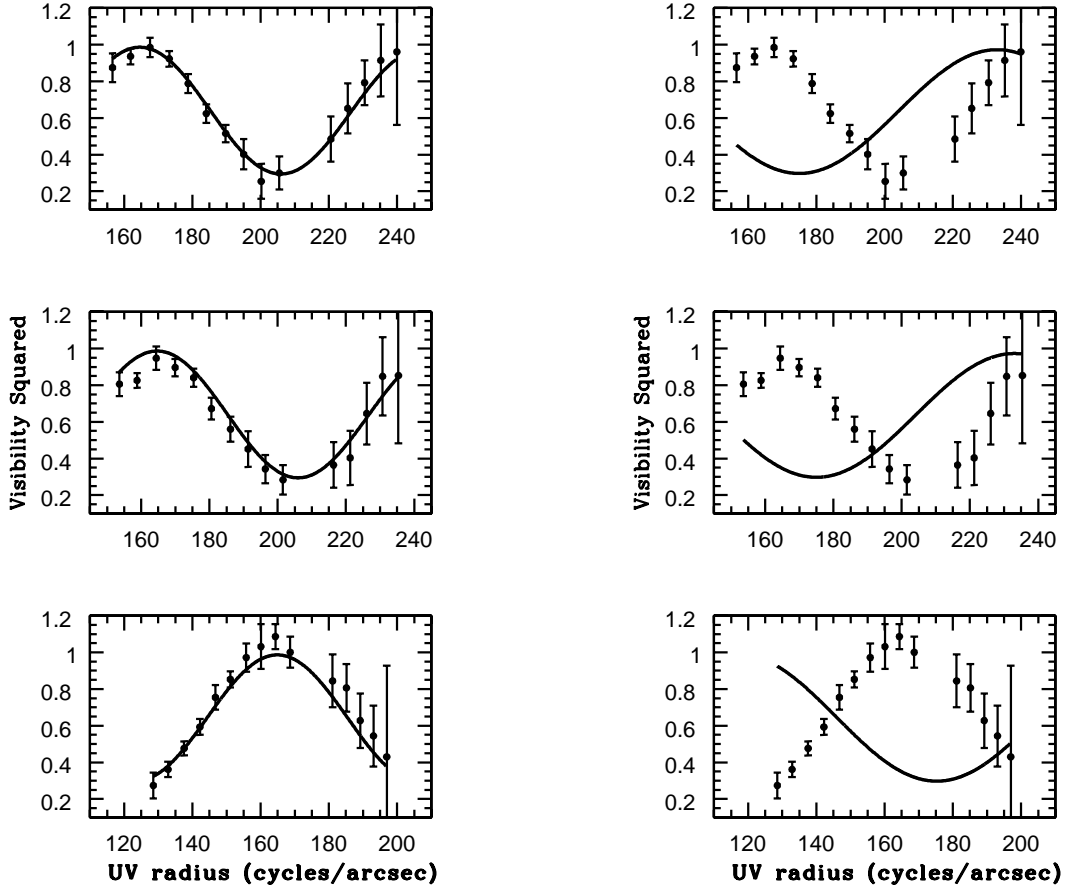


Fig. 1.— Left: Panels showing 3 of 9 scans of the calibrated V^2 of θ^1 Ori C observed with the AE-AW baseline on 2007 Mar 06 overlaid with a model of separation 12.17 mas and position angle 86.6° (Table 1). Right: A set of three panels shows the same data but overlaid using the predicted separation of 8.6 mas at a position angle of 86.28° for orbit 1 of Kraus et al. (2007) on that date. The errors include both a statistical error and an estimate of the uncertainty of the calibration.

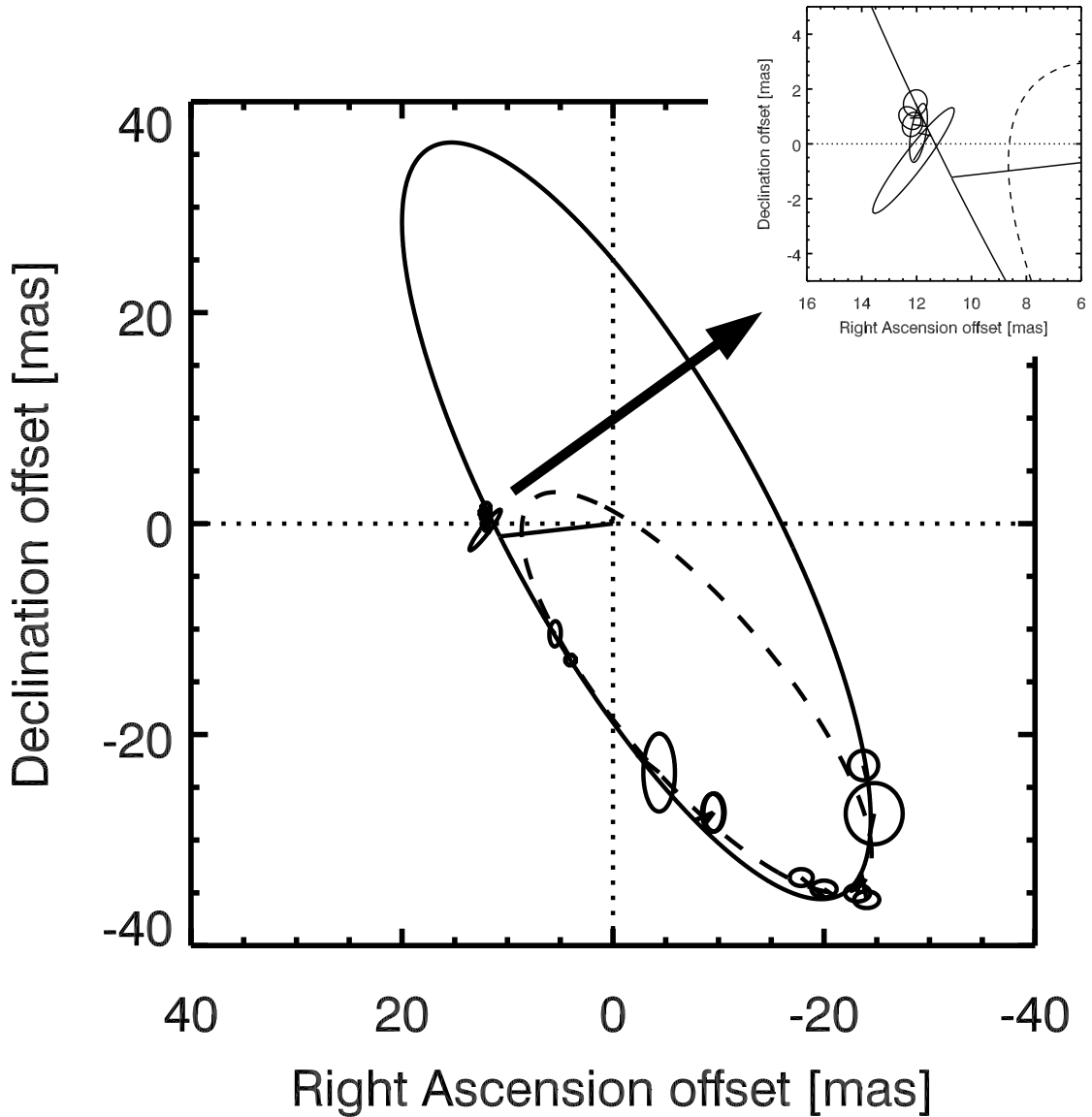


Fig. 2.— The best-fit orbit of θ^1 Ori C with orbital elements listed in Table 2 is plotted as a solid line. This fit incorporates the NPOI astrometric results from Table 1 and previous measurements given in Kraus et al. (2007). Error ellipses for the astrometric points are shown along with a vector indicating the periastron point. The dashed line shows the predicted orbit (Orbit1) from Kraus et al. (2007). We display the closely spaced 2007 NPOI astrometric solutions in the inset for clarity. The next set of observations should demonstrate decisively the validity of a longer period solution.

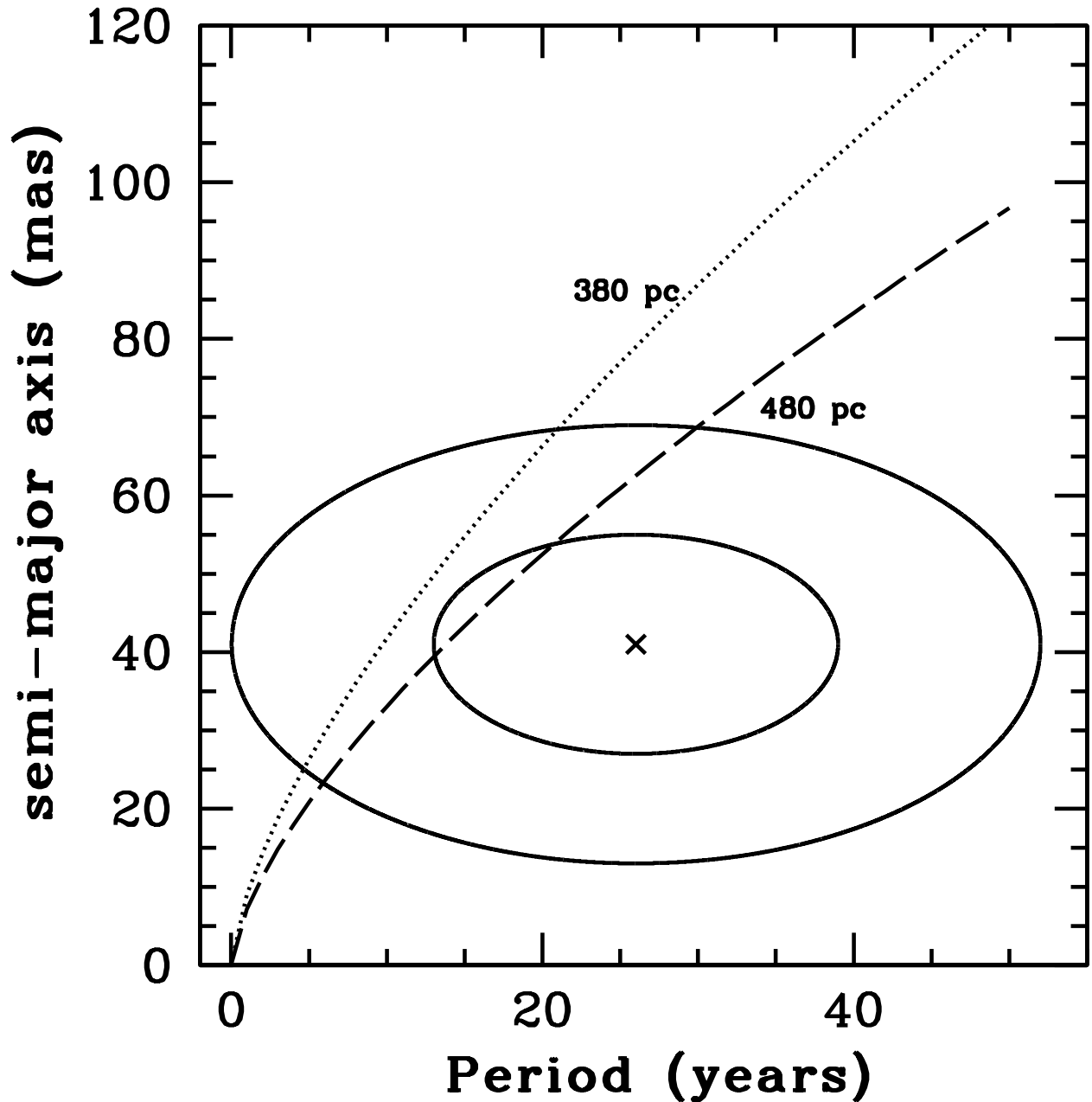


Fig. 3.— The best-fit period and semi-major axis from Table 2 are plotted with a cross, and the superimposed error ellipses (solid lines) represent the 1 and 2 σ errors of the orbital elements in Table 2. For a total system mass of 40 M_{\odot} , the period and semi-major axis values consistent with distances of 480 pc (dashed) and 380 pc (dotted) are also indicated. At the $\sim 1 \sigma$ level, the current orbit fit is consistent with essentially all measured distances to θ^1 Ori C. Given the limited phase coverage of the orbit a definitive distance measurement will require continued observations.